ChemComm

Accepted Manuscript

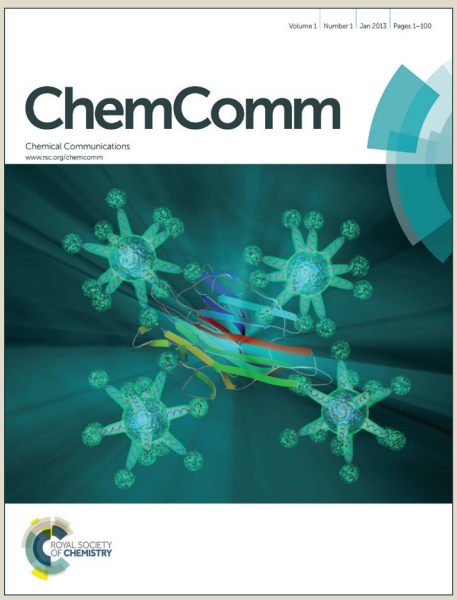

ROYAL SOCIETY OF CHEMISTRY

www.rsc.org/chemcomm

Cite this: DOI: 10.1039/c0xx00000x

www.rsc.org/xxxxxx

ARTICLE TYPE

Two Luminescent Zn(II) Metal–Organic Frameworks For Exceptionally Selective Detection of picric acid explosive

Zhi-Qiang Shi,[ab] Zi-Jian Guo[a] and He-Gen Zheng*[a]

Received (in XXX, XXX) Xth XXXXXXXXX 20XX, Accepted Xth XXXXXXXXX 20XX

DOI: 10.1039/b000000x

Abstract: Two luminescent Zn(II) metal–organic frameworks were prepared from a π-conjugated thiophene-containing carboxylic acid ligand. These two MOFs show strong luminescene and their luminescence could be quenched by a series of nitroaromatic explosives. Importantly, they exhibit very highly sensitive and selective detection of picric acid compared to other nitroaromatic explosives.

Recently fluorescent molecular assemblies such as polymers, gels and metal–organic frameworks[1] (MOFs) have been exploited for the detection of nitroaromatic explosives[2], due to the increasing concern over environment security. Compared with traditional methods for detection of nitroaromatic explosives, such as gas chromatography, Raman spectroscopy, ion mobility spectrometry, and other analysis methods, MOFs-based fluorescence detection shows great advantages because of their easy synthesis, low cost, electronic tenability, easy portability and operability. In most cases, the detection mechanism is an oxidative quenching mechanism.[2a, 2e] That is to say, upon photo-excitation, the electrons transfer from MOFs acting as electron donors to the electron-deficient nitroaromatic analytes causing the formation of oxidation of the excited state and the luminescence quenching. So, utilizing electron-rich π-conjugated fluorescent ligands is an effective strategy to construct MOFs that can act as very efficient luminescent sensors. Up to date, although a large number of luminescent MOFs have been synthesized and employed for explosives detection, the selective detection of one nitro explosive in the presence of others has not been well investigated. Still there is much more interest to discover new luminescent MOFs for selective detection of special one nitro explosive other than all the explosives.

Herein, we report the synthesis of two luminescent MOFs, $[Zn_2(L)_2(dpyb)]$ (**MOF-1**) and $[Zn(L)(dipb)]\cdot(H_2O)_2$ (**MOF-2**) (H_2L= 3,3'-(thiophene-2,5-diyl)dibenzoic acid (Supporting Information), dpyb = 1,4-di(pyridin-4-yl)benzene, dipb = 4,4'-di(1H-imidazol-1-yl)-1,1'-biphenyl), both of which exhibit highly selective responses towards picric acid comparing to other nitroaromatic explosives. Choosing H_2L as the main ligand is based on two major considerations: 1) H_2L is a π-conjugated thiophene-containing fluorescent ligand with rich electron and good electron-transferring ability. 2) The rotation of the C–C single bonds between thiophene and benzene rings can adjust the coordination orientation of the carboxylic acids. So, the MOFs constructed by H_2L ligand can display varied topological structures and expected luminescent properties for nitroaromatic explosives detection.

Single crystals of **MOF-1** and **MOF-2** suitable for X-ray diffraction studies were obtained by the solvothermal reaction of H_2L, $Zn(NO_3)_2\cdot6H_2O$ and dpyb (or dipb) in DMA/H_2O (DMA = N,N-dimethylacetamide; detailed procedure given in the ESI†).

Single-crystal X-ray diffraction analysis reveals that **MOF-1** crystallizes in the triclinic crystal system with space group of *P*-1. As shown in Fig. S2a (ESI†), the Zn(II) cation locates in a $\{ZnNO_4\}$ distorted square-pyramidal geometry made up of one N atoms [Zn-N = 2.061(3) Å] from the dpyb ligand and four oxygen atoms [Zn-O = 2.034(3) - 2.063(3) Å] from two symmetrical L ligands. The dihedral angles between the thiophene and two benzene rings of the L ligand are 24.91(0.17)° and 55.37(0.19)°, respectively, and the dihedral angle between the two benzene rings is 74.00(0.16)°. Two crystallographically equivalent Zn(II) cations are bridged by four carboxylate groups which adopt a bis-bidentate coordination mode to form a dinuclear Zn(II) "paddlewheel" secondary building unit (SBU) with a Zn···Zn distance of 2.9775(10) Å. Such SBUs are bridged by dpyb ligands to form a 2D (4, 4)-sql network with rhomb-like windows with the dimentions about 7.324 × 13.430 $Å^2$ (Fig. S2b). Interestingly, the spacer ligand dpyb from the adjacent layer penetrates the rhomb ring $[Zn_2(L)_2]$ to form a rotaxane structure. Due to rotaxane type arrangement, it generates 2-fold entanglement (Figs. 1a and S2c). Such polyrotaxane entanglements are rare.[2c] Furthermore, adjacent two sets of the entanglements are connected through C–H···π stacking, generating a 3D supramolecular motif (Fig. S2d).

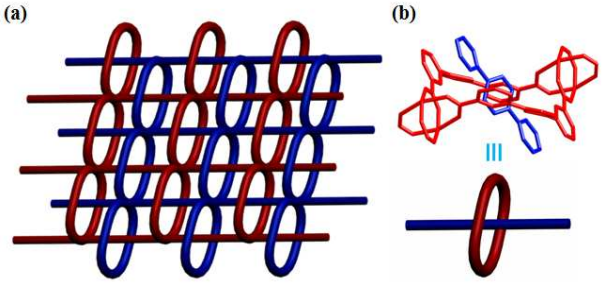

Fig. 1 (a) The schematic presentation of 2-fold interpenetrated layer structure of **MOF-1.** (b) The relative alignments of wheel and axle in **MOF-1.**

Single-crystal X-ray determination shows that **MOF-2** crystallizes in the orthorhombic crystal system with space group of *P*bca. The coordination geometry around the Zn(II) cation is depicted in Fig. S3a. The Zn(II) cation is coordinated by two N atoms [Zn-N = 2.001(3) - 2.014(3) Å] from two symmetrical dipb ligands and two oxygen atoms [Zn-O = 1.962(2) - 1.977(3) Å] from two symmetrical L ligands, and adopts a slightly distorted $\{ZnN_2O_2\}$ tetrahedral

geometry. Different from the case for **MOF-1**, the carboxylate groups act as monodentate mode. It is noteworthy that the dihedral angles formed by thiophene and benzene rings of the L ligand are quite different from **MOF-1**, which are 3.18(0.22)°, 1.78(0.22)° and 2.02(0.23)°. As shown in Fig. S3b, **MOF-2** is a 3D framework structure. Topological analysis[3] was employed to better insight of the **MOF-2**, the Zn(II) cations can be regarded as 4-connected nodes, and all the organic ligands are considered as linkers, the framework of **MOF-2** can be simplified to a classical 4-connected diamond (**dia**) with Schläfli symbol $\{6^6\}$. In order to minimize the void space in the single net, two equivalent nets adopt 2-fold interpenetration (Figure 2). After interpenetration, the structure only retains 7.8% solvent accessible void volume calculated by PLATON.[4]

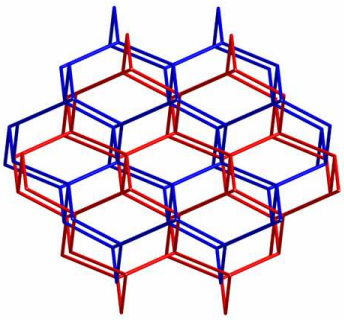

Fig. 2 The 2-fold interpenetrated dia topology of **MOF-2**.

MOFs constructed from d^{10} metal centers and π-conjugated ligands are promising to have excellent photoluminescent properties. Therefore, the luminescent properties of the two compounds and free ligand H_2L were measured in the solid state (λ_{ex} = 382 nm). **MOF-1** and **MOF-2** show strong emission peaks appear at 533 nm and 523 nm, respectively (Fig. S6). Compared with the free ligand H_2L, the emissions of **MOF-1** and **MOF-2** may originate from the intraligand fluorescent emission of the H_2L ligand. The strong emissions of **MOF-1** and **MOF-2** in solid state make it possible to use them in fluorescence detection. So, the photoluminescence of **MOF-1** and **MOF-2** were investigated in different organic solvents to examine the potentials of sensing of small molecules. 1 mg of **MOF-1** or **MOF-2** was finely ground down and then immersed in 2 mL of different organic solvents. After treatment by ultrasonication for 2h, the mixtures were aged for 3 days in order to form stable suspensions before the fluorescence measurements. The organic solvents used are DMA, DMF, methanol, ethanol, acetonitrile, acetone, tetrahydrofuran (THF), trichloromethane ($CHCl_3$), dichloromethane (CH_2Cl_2), and nitrobenzene. As shown in Fig. S7, the photoluminescence intensities are strongly dependent on the organic solvents. Both **MOF-1** and **MOF-2** show the strongest emissions in DMA. In contrast, the nitrobenzene emulsions display completely quenching effect. Such solvent-dependent luminescent properties inspired us to investigate the possibility of sensing other nitroaromatic explosives. To examine sensing sensitivity toward nitroaromatic explosives, including picric acid (PA), 4-nitrophenol (4-NP), 3-nitrophenol (3-NP), 2,4-dinitrophenol (2,4-DNP), nitrobenzene (NB), 1,4-nitrotoluene (NT), 1,3-dintrobenzene (1,3-DNB), 1,4-dintrobenzene (1,4-DNB), and 2,4-dinitrotoluene (2,4-DNT), in detail, a series of suspensions of **MOF-1** and **MOF-2** in DMA with gradually increasing the concentrations of nitroaromatic explosives in DMA solution (5 mM) were prepared to monitor the photoluminescence response. As shown in Fig. 3, the photoluminescence intensities decrease sharply with the increase of PA solution to DMA emulsion of **MOF-1** and **MOF-2**.

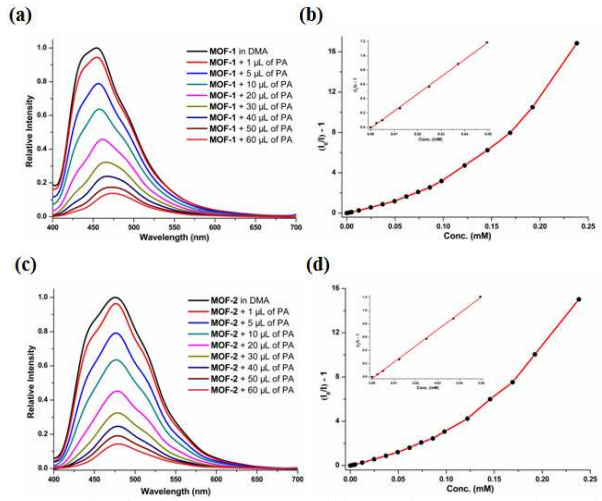

Fig. 3 (a) Photoluminescent spectra and (b) SV plot of **MOF-1** by gradual addition of 5 mM PA in DMA. (c) Photoluminescent spectra and (d) SV plot of **MOF-2** by gradual addition of 5 mM PA in DMA. The insets show the emission quenching linearity relationship at low concentrations of PA.

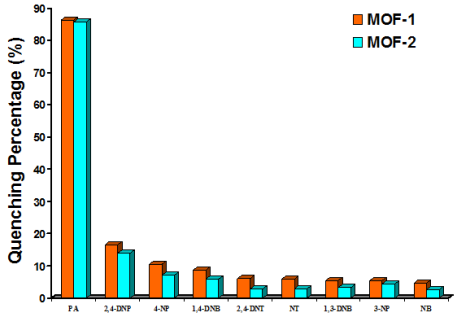

Fig. 4 Percentage of photoluminescence quenching of **MOF-1** and **MOF-2** upon addition of different explosive analytes.

The photoluminescence intensity decreased to 13.80 % for **MOF-1** and 14.29 % for **MOF-2**, respectively, only upon incremental addition of 60 μL PA solution (Fig. 4). The photoluminescence quenching by PA could be determined at low concentration (2.5 μM; Figs. 3a and 3c) for both the MOFs, which is comparable to or better than the previously reported photoluminescence sensor for PA.[5] Another interesting point is that the other nitroaromatic explosives show minor effects on the photoluminescence intensity of **MOF-1** and **MOF-2** (Figs. S8a-S23a). Such results indicate that both MOFs have high selectivity for PA compared to other nitroaromatic explosives (Fig. 4). The photoluminescence quenching efficiency can be quantitatively explained by the Stern-Volmer (SV) equation: $(I_0/I) = 1 + K_{sv}[Q]$, in which K_{sv} is the quenching constant (M^{-1}), [Q] is the molar concentration of the nitro analyte, I_0 and I are the photoluminescence intensities before and after addition of the nitro analyte, respectively. The Stern-Volmer plots for PA are nearly linear at low concentrations (R^2 = 0.9989 for **MOF-1** and 0.9985 for **MOF-2**) (Figs. 3b and 3d). The plots subsequently deviate from linearity and bend upwards at higher concentrations (Figures 3b and 3d). Such phenomena of nonlinear SV plots may be due to self-absorption or an energy-transfer process.[5b, 6] While all the other nitroaromatic explosives display nearly linear SV plots (Figs. S8b-S23b). Both **MOF-1** and **MOF-2** show the highest K_{sv} values with PA, at 2.40 × 10^4 and 2.46 × 10^4 M^{-1}, respectively, which are comparable to those of known organic polymers.[7] While the K_{sv} values calculated for the other

nitroaromatic explosives are much lower (Table S3). For **MOF-1** and **MOF-2**, the quenching constants for PA are ca. 68 and 106 times greater than for NB, respectively. To the best of our knowledge, these values are the highest for the known luminescent MOF-based sensors. The high quenching constants and the low detection concentrations for PA indicate easy identification the existence of a trace quantity of explosive. In addition, both the MOFs also respond rapidly and sensitively to the PA vapor, which is little lower than the solution. Within 1 min, a quenching maximum percentage of approximately 80% was reached (Figs. S24 and S25).

To better understand the high selectivity of the two MOFs towards PA, the quenching mechanism was investigated. Because of highly localized electronic states, MOFs constructed from d^{10} metal ions are often characterized by narrow energy bands. So, their valence band (VB) and conduction band (CB) energy levels can be described in a way similar to molecular orbitals (MOs).[2o] As discussed above, the photoluminescence of **MOF-1** and **MOF-2** originate from the intraligand of H_2L ligand. The electron-rich property of the H_2L ligand gives a higher LUMO energy than the LUMOs of nitro analytes. This can force the excited state electrons transfer from the CB of the MOF to the LUMOs of the nitro analytes, thus resulting in fluorescence quenching upon excitation. The isodensity surfaces and energy levels of the HOMO and LUMO orbitals computed by density functional theory at the B3LYP/6-31G(d) level for the H_2L ligand and nitro analytes are shown in Fig. S22. The maximum quenching observed for PA is in accord with the LUMO energies of nitro analytes. The absorption band intensities at 296 nm and 295 nm reduced (Fig. S27), and new absorption bands at 363 nm and 362 nm were observed, indicating the formation of charge transfer complexes upon addition of PA. But, the order of observed quenching efficiency is not fully in agreement with the corresponding LUMO energies of the other nitro analytes. This indicates that electron transfer is not the only mechanism for quenching. Another possible reason for the quenching maybe resonance energy transfer mechanism.[2b, 5a, 8] The nonlinearity of SV plot for PA suggests that such energy transfer mechanism exists in the photoluminescence quenching progress. If the absorption band of the nitro analyte has an effective overlap with the emission spectrum of the MOFs, the resonance energy can transfer from the MOFs to the nitro analyte. Therefore, the photoluminescence quenching efficiency and sensitivity can be significantly improved.[9] As exhibited in the UV-vis absorption spectra (Fig. S28), the absorption band of PA has the greatest degree of overlap with the photoluminescence spectra of **MOF-1** and **MOF-2** in DMA, while all of the other nitro analytes almost have no overlap. As a result, the coexistence of electron transfer and resonance energy transfer makes PA exhibiting high photoluminescence quenching compared to other nitro analytes.

In conclusion, two photoluminescent Zn(II) MOFs have been successfully synthesized for sensitive detection of nitroaromatic explosives through photoluminescent quenching. Notably, both the MOFs exhibit highly selective detection of PA. The quenching mechanism for such high selectivity is due to the electron and resonance energy transfer. The present work provides a new strategy to rational design and synthesis MOF-based sensors for selective detection of one nitro explosive from other nitro explosives.

This work was supported by grants from the Natural Science Foundation of China (Nos. 21371092; 91022011), National Basic Research Program of China (2010CB923303).

Notes and references

[a] *State Key Laboratory of Coordination Chemistry, School of Chemistry and Chemical Engineering, Collaborative Innovation Center of Advanced Microstructures, Nanjing University, Nanjing 210093, P. R. China, E-mail: zhenghg@nju.edu.cn. Fax: +86-25-83314502.*
[b] *College of Chemistry and Chemical Engineering, Taishan University, Taian 271021, P.R. China*

† Electronic Supplementary Information (ESI) available: Experiment details, additional figures, FT-IR spectra, TGA curves, photoluminescent spectra, SV plots, tables and X-ray structural datas. CCDC numbers 1035800 and 1035802 for **MOF-1** and **MOF-2**.

1 (*a*) K. K. Kartha, A. Sandeep, V. C. Nair, M. Takeuchi and A. Ajayaghosh, *Phys. Chem. Chem. Phys*., 2014, **16**, 18896-18901; (*b*) K. K. Kartha, S. S. Babu, S. Srinivasan and A. Ajayaghosh, *J. Am. Chem. Soc*., 2012, **134**, 4834-4841; (*c*) J. R. Long and O. M. Yaghi, *Chem. Soc. Rev*., 2009, **38**, 1213-1214.

2 (*a*) J. Ye, L. Zhao, R. F. Bogale, Y. Gao, X. Wang, X. Qian, S. Guo, J. Zhao and G. Ning, *Chem.–Eur. J.*, 2015, **21**, 2029-2037; (*b*) B. Joarder, A. V. Desai, P. Samanta, S. Mukherjee and S. K. Ghosh, *Chem.–Eur. J.*, 2015, **21**, 965-969; (*c*) I.-H. Park, R. Medishetty, J.-Y. Kim, S. S. Lee and J. J. Vittal, *Angew. Chem. Int. Ed*., 2014, **53**, 5591-5595; (*d*) X.-Z. Song, S.-Y. Song, S.-N. Zhao, Z.-M. Hao, M. Zhu, X. Meng, L.-L. Wu and H.-J. Zhang, *Adv. Funct. Mater.,* 2014, **24**, 4034-4041; (*e*) B. Gole, A. K. Bar and P. S. Mukherjee, *Chem.–Eur. J.*, 2014, **20**, 2276-2291; (*f*) G.-Y. Wang, C. Song, D.-M. Kong, W.-J. Ruan, Z. Chang and Y. Li, *J. Mater. Chem. A*., 2014, **2**, 2213-2220; (*g*) J.-S. Qin, S.-J. Bao, P. Li, W. Xie, D.-Y. Du, L. Zhao, Y.-Q. Lan and Z.-M. Su, *Chem.–Asian. J.*, 2014, **9**, 749-753; (*h*) Y.-C. He, H.-M. Zhang, Y.-Y. Liu, Q.-Y. Zhai, Q.-T. Shen, S.-Y. Song and J.-F. Ma, *Cryst. Growth Des.*, 2014, **14**, 3174-3178; (*i*) Y.-S. Xue, Y. He, L. Zhou, F.-J. Chen, Y. Xu, H.-B. Du, X.-Z. You and B. Chen, *J. Mater. Chem. A*., 2013, **1**, 4525-4530; (*j*) Y.-W. Li, J.-R. Li, L.-F. Wang, B.-Y. Zhou, Q. Chen and X.-H. Bu, *J. Mater. Chem. A*., 2013, **1**, 495-499; (*k*) G.-Y. Wang, L.-L. Yang, Y.Li, H. Song, W.-J. Ruan, Z. Chang and X.-H. Bu, *Dalton Trans*., 2013, **42**, 12865-12868; (*l*) S. Pramanik, Z. Hu, X. Zhang, C. Zheng, S. Kelly and J. Li, *Chem.–Eur. J.*, 2013, *19*, 15964-15971; (*m*) S. Pramanik, C. Zheng, X. Zhang, T. J. Emge and J. Li, *J. Am. Chem. Soc*., 2011, **133**, 4153-4155; (*n*) B. Gole, A. K. Bar and P. S. Mukherjee, *Chem. Commun*., 2011, **47**, 12137-12139; (*o*) A. Lan, K. Li, H. Wu, D. H. Olson, T. J. Emge, W. Ki, M. Hong and J. Li, *Angew. Chem. Int. Ed*., 2009, **48**, 2334-2338.

3 V. A. Blatov, A. P. Shevchenko, V. N. Serezhkin, *J. Appl. Crystallogr.*, 2000, **33**, 1193.

4 A. L. Spek, Platon Program, *Acta Crystallogr*,. *Sect. A*: *Fundam. Crystallogr*., 1990, **46**, 194.

5 (*a*) X. Jiang, Y. Liu, P. Wu, L. Wang, Q. Wang, G. Zhu, X.-l. Li and J. Wang, *RSC Adv*., 2014, **4**, 47357-47360; (*b*) S. S. Nagarkar, B. Joarder, A. K. Chaudhari, S. Mukherjee and S. K. Ghosh, *Angew. Chem. Int. Ed.*, 2013, **52**, 2881-2885.

6 (*a*) Q. Zhang, A. Geng, H. Zhang, F. Hu, Z.-H. Lu, D. Sun, X. Wei and C. Ma, *Chem.–Eur. J.*, 2014, **20**, 4885-4890; (*b*) S.-R. Zhang, D.-Y. Du, J.-S. Qin, S.-J. Bao, S.-L. Li, W.-W. He, Y.-Q. Lan, P. Shen and Z.-M. Su, *Chem.–Eur. J.*, 2014, **20**, 3589-3594; (*c*) Y. Salinas, R. Martinez-Manez, M. D. Marcos, F. Sancenon, A. M. Castero, M. Parra and S. Gil, *Chem. Soc. Rev*., 2012, **41**, 1261-1296; (*d*) W. Wu, S. Ye, G. Yu, Y. Liu, J. Qin and Z. Li, *Macromol. Rapid Commun*., 2012, **33**, 164-171; (*e*) D. Zhao and T. M. Swager, *Macromolecules*, 2005, **38**, 9377-9384; (*f*) H. Sohn, M. J. Sailor, D. Magde and W. C. Trogler, *J. Am. Chem. Soc.*, 2003, **125**, 3821-3830.

7 (*a*) J. C. Sanchez, A. G. DiPasquale, A. L. Rheingold and W. C. Trogler, *Chem. Mater*., 2007, **19**, 6459-6470; (*b*) A. Saxena, M. Fujiki, R. Rai and G. Kwak, *Chem. Mater*., 2005, **17**, 2181-2185.

8 S. S. Nagarkar, A. V. Desai and S. K. Ghosh, *Chem. Commun*., 2014, **50**, 8915-8918.

9 (*a*) W. Wei, X. B. Huang, K. Y. Chen, Y. M. Tao and X. Z. Tang, *RSC Adv*., 2012, **2**, 3765-3771; (*b*) J. Wang, J. Mei, W. Z. Yuan, P. Lu, A. J. Qin, J. Z. Sun, Y. G. Ma and B. Z. Tang, *J. Mater. Chem*., 2011, **21**, 4056-4059.

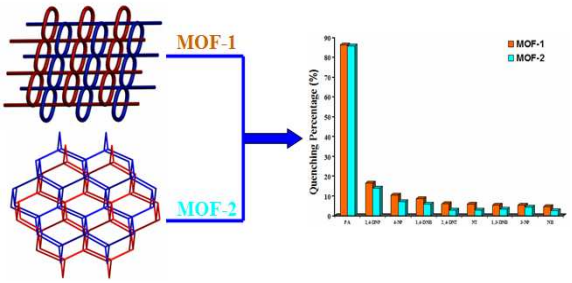

Two luminescent thiophene-containing Zn–MOFs exhibit very highly sensitive and selective detection of picric acid compared to other nitroaromatic explosives.